Available online at www.sciencedirect.com
ScienceDirect
Fluid Phase Equilibria 256 (2007) 20–26
FLUID PHASE EQUILIBRIA
www.elsevier.com/locate/fluid

Density functional study on the osmotic coefficient for the DNA–electrolyte solutions

Yang-Xin Yu [a,b,*], Ke Wang [a,b], Guang-Hua Gao [a,b]

[a] *Department of Chemical Engineering, Tsinghua University, Beijing 10084, PR China*
[b] *State Key Laboratory of Chemical Engineering, Tsinghua University, Beijing 100084, PR China*

Received 23 June 2006; received in revised form 21 September 2006; accepted 21 September 2006
Available online 1 November 2006

Abstract

The ion density profiles and mean electrostatic potentials around DNA from the Monte Carlo simulations are compared with the predictions of the Poisson–Boltzmann equation and the density functional theory. The DNA molecules are modeled as a charged cylinder while the ions are represented as charged hard spheres with different diameter. In the density functional theory, the Helmholtz free energy functional due to hard-sphere repulsion and electrostatic interaction are obtained from the modified fundamental measure theory and a quadratic functional Taylor expansion, respectively. The results show that due to the inclusion of the ion–ion correlation, the density functional theory is more accurate than the Poisson–Boltzmann equation. The density functional theory gives accurate ion structures and mean electrostatic potentials near the surface of DNA. When the established density functional theory is combined with the cell model, the osmotic coefficients of aqueous DNA–electrolyte solutions can be predicted. The results show that the DFT-cell model captures the essential features of the experimental osmotic coefficient, but fails to give a quantitative description. Possible reasons for this discrepancy are discussed.

Keywords: Osmotic coefficient; Density functional theory; DNA; Electrolyte solution

1. Introduction

The physical–chemical and biological properties of nucleic acids in an aqueous solution are strongly influenced by the strong electrostatic forces that depend on the type and concentration of counterions in solution [1]. The counterions in the immediate vicinity of a highly charged DNA polyanion are believed to be electrostatically associated, rather than immobilized at specific sites. A detailed investigation of the osmotic properties and the spatial distribution of mixed-size counterions in the vicinity of the surface of DNA will lead to a macro- and microscopic understanding of the DNA–electrolyte solution.

Computer simulation studies and various theoretical explorations have been carried out for the structures and thermodynamic properties of counterions around DNA in aqueous solutions. It is simple and popular to model DNA as infinitely long rigid charged cylinder, although more realistic models have also been studied. Ten years ago, Jayaram and Beveridge [2] provided a good review of the theoretical and computational investigations of the ion atmosphere of DNA as related to issues of both structure and function. In their review, Manning's elementary yet elegant concept of "counterion condensation" (CC) is revisited and shown to be good in several problems including analyses of competitive binding equilibria [3]. Another classical theory known as Poisson–Boltzmann (PB) equation is also widely used in this field. The PB equation can be solved either analytically for simple geometries, or numerically for more complicated physical models such as all-atom model of DNA, etc. [2]. This approximation is adequate for dilute solution of monovalent cations but leads to bad results for the systems at high bulk concentration or involving multivalent cation due to its neglect of the excluded volume effect and correlation between small ions [4–6]. To consider the exclude volume effect and ion correlation, several theoretical approaches are proposed. These approaches including the hypernetted-chain/mean-spherical (HNC/MSA) [7], modified Poisson–Boltzmann theory [8,9]

* Corresponding author at: Department of Chemical Engineering, Tsinghua University, Beijing 10084, PR China. Tel.: +86 1062782558; fax: +86 1062770304.
E-mail address: yangxyu@mail.tsinghua.edu.cn (Y.-X. Yu).

0378-3812/$ – see front matter © 2006 Elsevier B.V. All rights reserved.
doi:10.1016/j.fluid.2006.09.029

and density functional theories [6,10] lead to a good description of the electrical double layer in various geometries, but most of them are limited to the restricted primitive model of electrolyte around DNA. Recently, we have extended the DFT to DNA–electrolyte solutions with the mixed-sized counterions and found that the DFT is fine for these systems [11].

In principle, any theories for the cylinder electric double layer can be properly combined with the cell model to predict the osmotic pressures or osmotic coefficients of DNA–electrolyte solutions [12-14]. For example, Blaul et al. [15] have used the Poisson–Boltzmann cell model to predict the osmotic coefficient of a synthetic stiff-chain polyelectrolyte solution without added salt. However, there is no report on the combination of the DFT with cell model. To investigate the applicability of the DFT-cell model to the osmotic coefficient of DNA–electrolyte solution, we present a DFT and carry out Monte Carlo simulations for the systems with mixed-size counterions. Comparisons of the results from the DFT with those from the Monte Carlo (MC) simulations are made and then the DFT are combined with the cell model to predict osmotic coefficient of aqueous DNA–electrolyte solutions.

2. Theory

2.1. Molecular model

The DNA molecule is modeled as an infinitely long, impenetrable charged cylinder. The radius of the hard cylindrical core of the DNA is R. We assume that there is a uniform charge distribution on the surface of DNA with a magnitude $e/2\pi Rb$, where e denotes charge of electron and b is the inverse of linear charge density on the DNA molecules. All ions are modeled as charged hard spheres with various diameters σ_α, and the minimal separation between ion α and axis of the DNA is $R+\sigma_\alpha/2$. The primitive model of electrolyte solution is used, i.e., the solvent water dielectric constant is $\varepsilon = 78.4$ at any position, corresponding to that of the pure water at $T = 298$ K. The ion-polyion interaction potential is given by

$$V_i^{\text{ext}}(r) = \begin{cases} -\dfrac{2e^2 z_i}{\varepsilon b} \ln r & r \geq R + \dfrac{\sigma_i}{2} \\ \infty & \text{otherwise} \end{cases} \tag{1}$$

where e denotes charge of electron, z_i and σ_i stand for valance and diameter of ion i, respectively, and r denotes the distance between axis of DNA and center of ion i.

The ion–ion interaction potential is given by

$$u_{ij} = \begin{cases} \dfrac{e^2 z_i z_j}{\varepsilon |\mathbf{r}_i - \mathbf{r}_j|} & |\mathbf{r}_i - \mathbf{r}_j| \geq \dfrac{\sigma_i + \sigma_j}{2} \\ \infty & \text{otherwise} \end{cases} \tag{2}$$

where $\mathbf{r}_i$ is the position of ion i.

The mean electrostatic potential $\psi(r)$ due to the uniform surface charge density at the surface of DNA as well as the internal ion distributions satisfies the corresponding Poisson equation. It can be derived from Poisson equation in one dimension and is given by [11]

$$\psi(r) = -\frac{4\pi e}{\varepsilon} \int_r^\infty \ln\left(\frac{r'}{r}\right) \sum_i \rho_i(r') z_i r' \, \mathrm{d}r' \tag{3}$$

with the electro-neutrality condition given by

$$2\pi b \int_R^\infty \mathrm{d}r \, r \sum_i \rho_i(r) z_i = 1 \tag{4}$$

where r and r' is the distance between the ion center and polyion axis, the subscript i denotes ion species i.

2.2. Density functional theory

The grand potential for ions with chemical potential μ_i in external potential $V_i^{\text{ext}}(\mathbf{r})$ is related to the Helmholtz energy functional for the ions through the Legendre transform:

$$\Omega[\{\rho_i(\mathbf{r})\}] = F[\{\rho_i(\mathbf{r})\}] + \sum_{i=1}^{N} \int \mathrm{d}\mathbf{r}[V_i^{\text{ext}}(\mathbf{r}) - \mu_i]\rho_i(\mathbf{r}) \tag{5}$$

where $\{\rho_i(\mathbf{r})\}$ is a set of density distributions for all small ions, N is the total number of ionic species, and $F[\{\rho_i(\mathbf{r})\}]$ represents the Helmholtz energy functional. At equilibrium, the grand potential reaches its minimum, i.e., $\delta\Omega[\{\rho_i(\mathbf{r})\}]/\delta\rho_i(\mathbf{r}) = 0$, and the Euler–Lagrange equation is obtained:

$$\mu_i - V_i^{\text{ext}}(\mathbf{r}) = \frac{\delta F[\{\rho_i(\mathbf{r})\}]}{\delta \rho_i(\mathbf{r})} \tag{6}$$

The key problem in a density functional theory is to find an analytical expression for the Helmholtz energy F as a functional of the density distributions. Without loss of generality, we may decompose F into four parts, i.e.:

$$F[\{\rho_i(\mathbf{r})\}] = F^{\text{id}} + F_{\text{hs}}^{\text{ex}} + F_C^{\text{ex}} + F_{\text{el}}^{\text{ex}} \tag{7}$$

where F^{id} is the ideal-gas contribution, $F_{\text{hs}}^{\text{ex}}$ the hard-sphere contribution, F_C^{ex} the direct Coulomb contribution and $F_{\text{el}}^{\text{ex}}$ represents a coupling of Coulombic and hard-sphere interactions. The ideal-gas contribution is given by the exact expression:

$$F^{\text{id}} = kT \sum_{i=1}^{N} \int \mathrm{d}\mathbf{r} \, \rho_i(\mathbf{r}) \left[\ln(\rho_i(\mathbf{r})\lambda_i^3) - 1\right] \tag{8}$$

where λ_i is the thermal de Broglie wavelength of component i and k is the Boltzmann constant. The direct Coulomb contribution is also known exactly, and is given by

$$F_{\text{C}}^{\text{ex}} = \frac{1}{2} \int\int \mathrm{d}\boldsymbol{r}_1 \, \mathrm{d}\boldsymbol{r}_2 \sum_{i,j} \frac{z_i z_j e^2 \rho_i(\boldsymbol{r}_1)\rho_j(\boldsymbol{r}_2)}{\varepsilon |\boldsymbol{r}_1 - \boldsymbol{r}_2|} \tag{9}$$

To find expressions for $F_{\text{hs}}^{\text{ex}}$ and $F_{\text{el}}^{\text{ex}}$ (both are ignored in the PB theory), we use a modified fundamental measure theory (MFMT) [16] developed recently and a quadratic expansion

of the Helmholtz energy functional, respectively. According to MFMT [16], the hard-core Helmholtz energy functional $F_{\rm hs}^{\rm ex}[\{\rho_i\}]$ is given by

$$\beta F_{\rm hs}^{\rm ex} = \int \Phi^{\rm hs}[n_\alpha(\boldsymbol{r})]\,{\rm d}\boldsymbol{r} \tag{10}$$

where $\beta = 1/k_{\rm B}T$, $n_\alpha(\mathbf{r})$ is the weighted density and defined as [16]:

$$n_\alpha(\boldsymbol{r}) = \sum_i \int \rho_i(\boldsymbol{r}')w_i^{(\alpha)}(|\boldsymbol{r}'-\boldsymbol{r}|)\,{\rm d}\boldsymbol{r}' \tag{11}$$

where $\alpha = 0, 1, 2, 3, {\rm V1}$ and V2, denoting the index of six weight functions $w_i^{(\alpha)}(r)$. The six weight functions are given by

$$w_i^{(2)}(r) = \pi\sigma_i^2 w_i^{(0)}(r) = 2\pi\sigma_i w_i^{(1)}(r) = \delta\left(\frac{\sigma_i}{2} - r\right) \tag{12}$$

$$w_i^{(3)}(r) = \theta\left(\frac{\sigma_i}{2} - r\right) \tag{13}$$

$$\mathbf{w}_i^{(2)}(\mathbf{r}) = 2\pi\sigma_i \mathbf{w}_i^{(1)}(\mathbf{r}) = \left(\frac{\mathbf{r}}{r}\right)\delta\left(\frac{\sigma_i}{2} - r\right) \tag{14}$$

where $\delta(r)$ is the Dirac delta function, $\theta(r)$ the Heaviside step function and $\Phi^{\rm hs}[n_\alpha(\mathbf{r})]$ is the reduced excess Helmholtz energy density due to hard-sphere repulsion, which can be expressed as

$$\Phi^{\rm hs}[n_\alpha(\mathbf{r})] = \Phi^{{\rm hs}(S)}[n_\alpha(\mathbf{r})] + \Phi^{{\rm hs}(V)}[n_\alpha(\mathbf{r})] \tag{15}$$

where the superscripts (S) and (V) stand for contributions from scalar and vector weighted densities, respectively. The scalar part is given by [16]:

$$\Phi^{{\rm hs}(S)}[n_\alpha(\mathbf{r})] = -n_0\ln(1-n_3) + \frac{n_1 n_2}{1-n_3} + \frac{n_2^3\ln(1-n_3)}{36\pi n_3^2} + \frac{n_2^3}{36\pi n_3(1-n_3)^2} \tag{16}$$

and the vector part is given by

$$\Phi^{{\rm hs}(V)}[n_\alpha(\mathbf{r})] = -\frac{\mathbf{n}_{\rm V1}\cdot\mathbf{n}_{\rm V2}}{1-n_3} - \frac{n_2\mathbf{n}_{\rm V2}\cdot\mathbf{n}_{\rm V2}}{12\pi n_3^2}\ln(1-n_3) - \frac{n_2\mathbf{n}_{\rm V2}\cdot\mathbf{n}_{\rm V2}}{12\pi n_3(1-n_3)^2} \tag{17}$$

In the limit of a bulk fluid, the two vector weighted densities $\mathbf{n}_{\rm V1}$ and $\mathbf{n}_{\rm V2}$ vanish, and the Helmholtz free energy density $\Phi^{\rm hs}$ becomes identical to that from the Boublik–Mansoori–Carnahan–Starling–Leland (BMCSL) equation of state.

Following the previous work on the DFT of electrical double layer, $F_{\rm el}^{\rm ex}$ can be obtained by making a functional Taylor expansion of the residual Helmholtz free energy functional around that for a uniform fluid [5,11,17]:

$$F_{\rm el}^{\rm ex} = F_{\rm el}^{\rm ex}[\{\rho_i^{\rm b}\}] + \int {\rm d}\boldsymbol{r}\sum_{i=1}^{N}\frac{\delta F_{\rm el}^{\rm ex}}{\delta\rho_i(\boldsymbol{r})}\Delta\rho_i(\boldsymbol{r}) + \int\int {\rm d}\boldsymbol{r}\,{\rm d}\boldsymbol{r}'\sum_{j=1}^{N}\sum_{i=1}^{N}\frac{\delta^2 F_{\rm el}^{\rm ex}}{\delta\rho_i(\boldsymbol{r})\delta\rho_j(\boldsymbol{r}')}\Delta\rho_i(\boldsymbol{r})\Delta\rho_j(\boldsymbol{r}') + \cdots \tag{18}$$

where $\{\rho_i^b\}$ is the set of all bulk densities and $\Delta\rho_i(\mathbf{r}) = \rho_i(\mathbf{r}) - \rho_i^{\rm b}$. According to the definition of direct correlation functions and neglecting all higher-order terms $\Delta C_{ijk}^{(n){\rm el}}$ $(n>2)$ in Eq. (18), $F_{\rm el}^{\rm ex}$ becomes:

$$\beta F_{\rm el}^{\rm ex} = \beta F_{\rm el}^{\rm ex}[\{\rho_i^{\rm b}\}] - \int {\rm d}\boldsymbol{r}\sum_{i=1}^{N}\Delta C_i^{(1){\rm el}}\,\Delta\rho_i(\boldsymbol{r}) - \iint {\rm d}\boldsymbol{r}\,{\rm d}\boldsymbol{r}'\sum_{i=1}^{N}\sum_{j=1}^{N}\Delta C_{ij}^{(2){\rm el}}(|\boldsymbol{r}'-\boldsymbol{r}|)\Delta\rho_i(\boldsymbol{r})\Delta\rho_j(\boldsymbol{r}') \tag{19}$$

The excess direct correlation function $\Delta C_{ij}^{(2){\rm el}}(r)$ can be obtained from, for example, numerical solutions of HNC or hybridized MSA closure of the Ornstein–Zernike equation. The most popular approach is to calculate $\Delta C_{ij}^{(2){\rm el}}(r)$ from the mean spherical approximation (MSA) [18,19] which yields analytical expressions in reasonable accuracy. In this work, the expression of $\Delta C_{ij}^{(2){\rm el}}(r)$ from the MSA is adopted.

From Eqs. (5)–(19), we can obtain the Euler–Lagrange equations for the density profiles of ions around DNA:

$$\rho_i(\boldsymbol{r}) = \rho_i^{\rm b}\exp\left\{\frac{1}{k_{\rm B}T}\left[-\frac{\delta F_{\rm hs}^{\rm ex}}{\delta\rho_i(\boldsymbol{r})} + \mu_{i,\boldsymbol{hs}}^{\boldsymbol{ex}}\right] - \frac{z_i e}{k_{\rm B}T}[\psi(\boldsymbol{r}) - \psi^{\rm b}] + \sum_{j=1}^{N}\int {\rm d}\boldsymbol{r}'\,\Delta C_{ij}^{(2){\rm el}}(|\boldsymbol{r}'-\boldsymbol{r}|)(\rho_j(\boldsymbol{r}') - \rho_j^{\rm b})\right\} \tag{20}$$

The Euler–Lagrange Eq. (20) can be solved by iterative numerical procedure to obtain the ion density profiles, where the weighted densities and integrals are evaluated numerically using a Gauss quadrature method. The initial guess for the iteration as well as the iteration procedure is similar to that described in detail in the paper of Gonzales-Tovar et al. [20].

3. Monte Carlo simulations

To test the density functional theory in a more extensive way, Monte Carlo simulations are carried out in canonical ensemble. A cylindrical simulation box with its axis coinciding with the axis of DNA molecule is used in our simulation. And the model is the same as described in Section 2.1. The radius and height of the simulation box are $R_{\rm box}$ and $H_{\rm box}$, respectively. A hard-wall outer boundary is imposed on the simulation box in radial direction, while a periodical boundary condition is applied in axial direction by imagining that the simulation box is replicated infinitely along the axial direction on both sides of the central box. In the calculation of the total energy of the system, if any ion overlaps with DNA molecule, radial outer boundary or other ions, the total energy of this configuration is positive infinite. Otherwise, the total energy of the system is calculated by

$$U_{\text{Total}} = -\sum_{i=1}^{N}\frac{2e^2 z_i}{\varepsilon b}\ln r_i + \sum_{i=1}^{N}\sum_{j>i}^{N}\frac{e^2 z_i z_j}{\varepsilon|\boldsymbol{r}_i - \boldsymbol{r}_j|_{\text{MI}}} + \sum_{i=1}^{N} e z_i \Phi_{\text{ext}}(\boldsymbol{r}_i) \quad (21)$$

The first term of right hand of Eq. (21) corresponds to the polyion–ion interaction, the second term is total electrostatic interactions between ions in central box calculated using minimum image (MI) criterion and $\boldsymbol{\Phi}_{\text{ext}}(\mathbf{r}_i)$ in the last term is external potential produced by the mobile ions out of central box. In the simulation, an iterative self-consistent method is used to correct the long-range energy, and another iterative algorithm is adopted to obtain desired bulk ionic concentration. The details of the simulation have been given in our previous work [11].

4. Results and discussion

4.1. Ion density distribution and mean electrostatic potential

An isolated model DNA molecule immersed in an electrolyte solution composed of two species of cations and one species of anion is considerd in this section. The radius of the hard cylindrical core of the DNA is $R = 0.8$ nm and parameter $b = 0.17$ nm. In Fig. 1, the ion density profiles around model DNA molecule predicted from the PB equation and present DFT are comparison with those from the canonical Monte Carlo simulations carried out in this work. In Fig. 1, the counterions are divalent and have different size. Similar to the restricted primitive model, there are significant accumulations of counterions near the surface of DNA, accompanied by a depletion of coions in the same region. The present DFT predicts very accurate density profiles of counterions but underestimates the density profile of coion. Compared with the MC data, the present DFT is more accurate than the nonlinear PB theory, especially for the density profiles of counterions near the DNA surface.

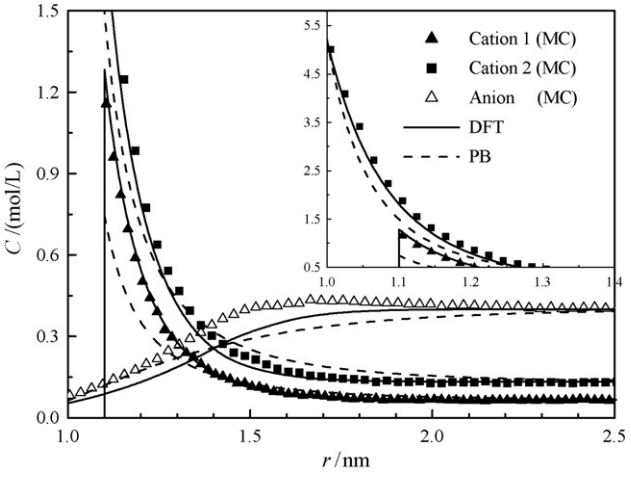

Fig. 1. Ion distributions around model DNA molecule predicted by the MC, DFT and PB equation. The electrolyte solutions contain two divalent cations (cations 1 and 2) and one monovalent anion. The diameters of both cation 2 and anion are fixed at 0.4 nm, and the diameter of cation 1 and the bulk concentrations of cations are $\sigma_{c1} = 0.6$ nm, $C^{b}_{c1} = 0.067$ mol/L, $C^{b}_{c2} = 0.133$ mol/L, respectively.

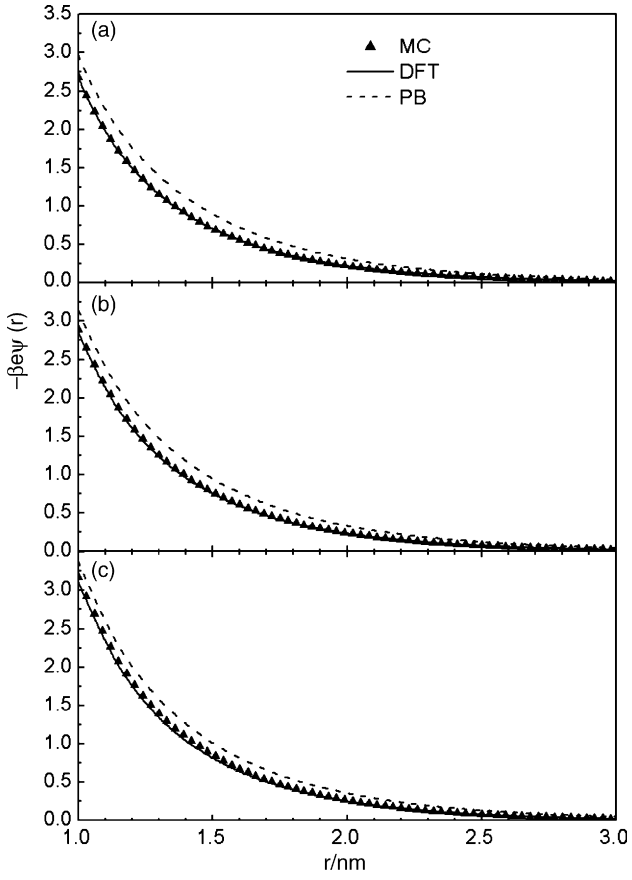

Fig. 2. Reduced mean electrostatic potential around DNA predicted by the MC, DFT and PB equation. The electrolyte solutions contain two monovalent cations and one monovalent anion. The diameters of cation 1, cation 2 and anion are fixed at 0.6, 0.4 and 0.4 nm, respectively. The total bulk concentration of cations is fixed at 0.300 M, but ratios of concentrations of cations 1–2 are (a) 1:5, (b) 1:1 and (c) 5:1.

Fig. 2 shows the dependence of electrostatic potential around DNA on the ratio of bulk concentration of two species of cations in monovalent cation systems. The results from the DFT agree quite well with those from MC simulations. The potential profiles predicted by the PB equation have obvious negative deviations from the MC simulation data, though the corresponding ion distributions only unnoticeably deviate from the MC results. Recall that the electrostatic potential is obtained by integrating the ion density distributions, the tiny deviations in ion density distributions will be accumulated and become noticeable in consequential electrostatic potentials. As shown in Fig. 2, the ratio of bulk concentration of two species of cations makes little contribution to the electrostatic potential, although it makes a strong impact on the corresponding microscopic structure of ions around DNA. The reason for this phenomenon is that the potential is an integral quantity, and some differences in density profiles are cancel each other out. Fig. 2 also indicates that at the fixed total concentration of cations the electrostatic potentials become slightly more negative when the concentration of larger cation increases.

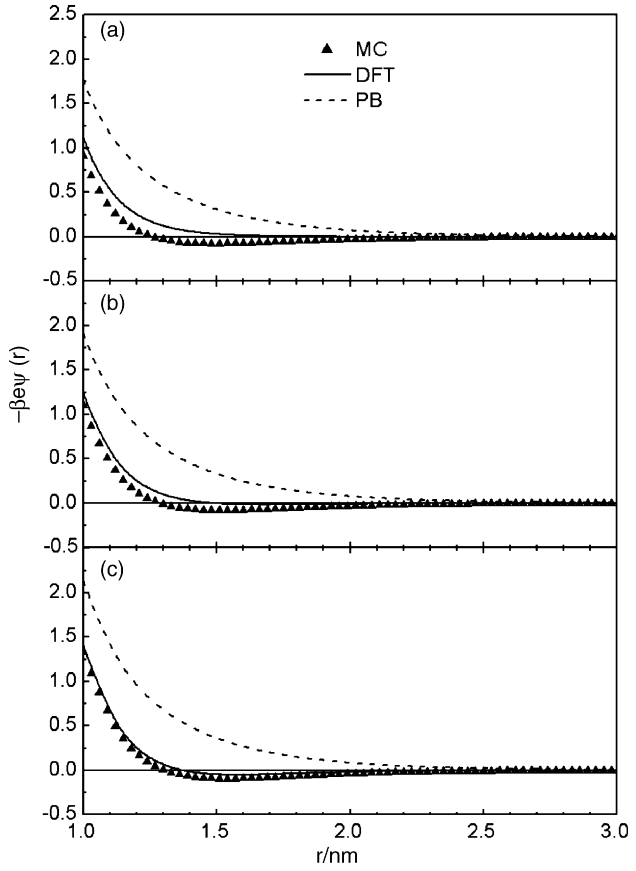

Fig. 3. Reduced mean electrostatic potential around DNA predicted by the MC, DFT and PB equation. The electrolyte solutions contain two divalent cations and one monovalent anion. The diameters of cation 1, cation 2 and anion are fixed at 0.6, 0.4 and 0.4 nm, respectively. The total bulk concentration of cations is fixed at 0.200 M, but ratios of concentrations of cations 1–2 are: (a) 1:4, (b) 1:1 and (c) 4:1.

The electrostatic potentials around DNA at three different ratios of bulk concentration of two species of divalent cations are plotted in Fig. 3. The difference between the predictions from the DFT and those from the MC simulations is larger than the case of monovalent cations. Comparing the three profiles presented in Fig. 3, one can see that as the bulk molar fraction of larger cation increases, the absolute value of the mean electrostatic potential increases slowly and the prediction from the DFT becomes more accurate.

We find from Fig. 3 that as the concentration of larger cation increases, or the diameter of one cation becomes larger, the prediction from DFT becomes accurate. Since the more content of the larger cations, the more contributions from the excluded volume effects, the above findings suggest that the hard-core repulsion contribution in the present DFT should be accurate and deviations from the simulations should be produced by the coupling of Columbic and hard-sphere interactions. That indicates the second direct correlation function used for asymmetric electrolyte contributes mainly to the total inaccuracy of the present DFT. It is also shown in Fig. 3 that the PB equation is not a good theory for the divalent cation system since it even hardly gives a qualitatively prediction of electrostatic potentials. Fig. 3 further validates that the second direct correlation function from MSA closure is not accurate for highly asymmetric electrolyte.

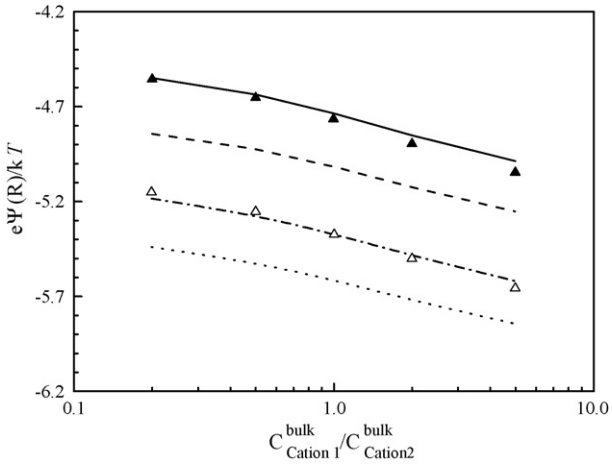

Fig. 4. Dependence of $\psi(R)$ on the bulk concentration ratios of two monovalent cations. The diameters of cation 1, cation 2 and anion are 0.6, 0.4 and 0.4 nm, respectively. The solid triangle, solid line and dashed line represent the results predicted by the MC, DFT and PB equation, respectively, for the system containing 0.300 mol/L cations. The open triangle, dash-dot line and dot line represent the results predicted by the MC, DFT and PB equation, respectively, for the system containing 0.150 mol/L cations.

The negatively charged groups on DNA surface and the surrounding mobile ions form an electric double layer around DNA. The local electrostatic potential varies along radial direction from R to infinity as shown Figs. 2 and 3. We now define the potential at R as $\psi(R)$. $\psi(R)$ is a typical value of electrostatic potential which reflects the extent that the surrounding small ions screen the electrostatic field produced by polyion. As a matter of fact, $\psi(R)$ should be negative infinity when the system is absent of small ions. Fig. 4 presents the dependence of $\psi(R)$ on ratio of the bulk concentrations of two cations. As shown in this figure, $\psi(R)$ becomes more negative as the bulk mole fraction of small cation decreases or as the total bulk cation concentration decreases. This suggests that the smaller the counterion is, or the more concentrated the bulk electrolyte solution is, the more the capacity of screening external electrostatic potential.

4.2. Osmotic coefficient

When the present DFT is combined with a cell model, it can be used to predict the osmotic coefficient of DNA–electrolyte solutions. The cell model osmotic coefficient can be calculated from the equation [12]:

$$\phi = \frac{\sum \rho_i(R_C)}{\sum \rho_i} \tag{22}$$

where $\rho_i(R_C)$ is the number density of ionic species i at the cell boundary, and ρ_i is the corresponding average number density in the solution.

Theoretical and experimental osmotic coefficients for salt-free DNA solution with monovalent counterion are compared in Fig. 5. In the calculation, $R = 0.8$ nm and $b = 0.17$ nm, corresponding to double-stranded DNA in B form [13], and the

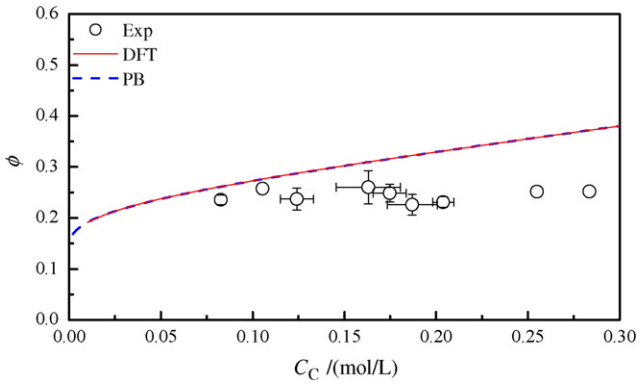

Fig. 5. The osmotic coefficient of salt-free DNA solution as a function of the counterion concentration (or DNA concentration) at 298.15 K. The symbols, dashed and solid lines represent the results of experiment [13], PB- and DFT-cell models.

counterion diameter $\sigma_C = 0.4$ nm, corresponding to Na^+. The PB-cell model and the present DFT-cell model have almost the same results in this case, overestimating the osmotic coefficient. Blaul et al. [15] pointed out the possible reasons for this discrepancy of PB-cell model is the neglect of the ion–ion correlations or specific interactions between the macroion and the counterions. However the DFT, which has included the ion–ion correlations, also gives too high osmotic pressure. In order to clarify this matter further, we calculate the osmotic coefficient of salt-free polystyrenesulfonate solution with mono- and trivalent counterions only and the results are plotted in Fig. 6. In Fig. 6, the polyion parameters are $R = 0.6$ nm and $b = 0.252$ nm, the diameters of both counterions are $\sigma_C = 0.4$ nm, and the equivalent fraction of the monovalent ions $\bar{N}_1$ is defined as

$$\bar{N}_1 = \frac{\rho_1}{3\rho_2 + \rho_1} \tag{23}$$

where ρ_1 and ρ_2 are, respectively, the average number densities of mono- and trivalent counterions in the polyion free volume of the cell. In this case the ion–ion correlation is strong, whereas we can see from Fig. 6 that DFT-cell model gives reasonable results for the osmotic coefficient. This indicates that the neglect of the

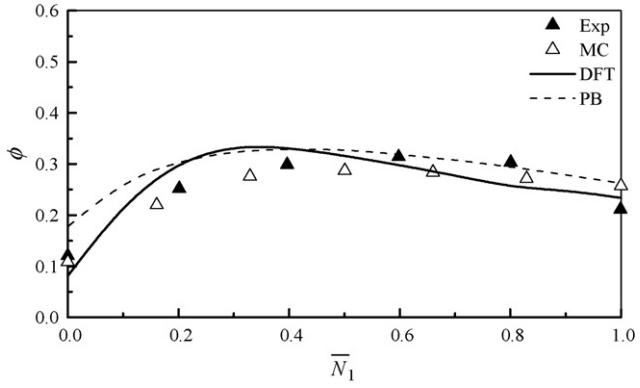

Fig. 6. The osmotic coefficient as a function of the equivalent fraction $\bar{N}_1$ for aqueous polystyrenesulfonate solution with mono- and trivalent counterions only at $C_p = 0.001$ mono mol/L and $T = 298$ K. Solid and opened triangles, dashed and solid lines represent the results from the experiment [22], Monte Carlo simulation [14], PB- and DFT-cell models, respectively.

ion–ion correlation is not the reason for the overestimation of osmotic coefficients for salt-free DNA solution, although including the ion–ion correlation may lower ϕ for the systems with divalent or trivalent counterions. Some additional specific interactions between DNA and the counterions, for example, binding of counterions to DNA, should be considered. In addition, the immediate neighborhood of DNA may exhibit a considerably lower dielectric constant than the bulk water, which leads to a stronger interaction between DNA and counterions [15,21].

5. Conclusions

In this paper, we have established a density functional theory to describe the ion distributions and mean electrostatic potentials around isolated DNA in mixed-size counterion solutions. Extensive comparison with the Monte Carlo simulation data suggest that the proposed DFT can be successfully used to predict the structures and the electrostatic potentials of ions in the vicinity of the surface of DNA and is superior to the well-known Poisson–Boltzmann theory. When the DFT is combined with the cell model, it predicts too high osmotic coefficient for the salt-free DNA solutions. A semi-quantitative fit of osmotic coefficient can be achieved by decreasing the parameter b. The small but significant discrepancy between the cell model and the experimental values may be traced back to the neglect of specific interactions between DNA and the counterions. A locally varying dielectric constant may lead to a better result for the estimation of the osmotic coefficient for DNA–electrolyte solutions.

Acknowledgements

We gratefully acknowledge the financial support from the National Natural Science Foundation of China (Project Grant No. 20376037).

References

[1] V.K. Misra, D.E. Draper, J. Mol. Biol. 294 (1999) 1135.
[2] B. Jayaram, D.L. Beveridge, Annu. Rev. Biophys. Biomol. Struct. 25 (1996) 367.
[3] M.T.J. Record, C.F. Anderson, T.M. Lohman, Q. Rev. Biophys. 11 (1978) 103.
[4] L. Degreve, M. Lozada-Cassou, Mol. Phys. 86 (1995) 759.
[5] Y.-X. Yu, J. Wu, G.-H. Gao, J. Chem. Phys. 120 (15) (2004) 7223.
[6] K. Wang, Y.-X. Yu, G.-H. Gao, Phys. Rev. E 70 (2004) 011912.
[7] L. Yeomans, S.E. Feller, E. Sanchez, M. Lozada-Cassou, J. Chem. Phys. 98 (2) (1993) 1436.
[8] L.B. Bhuiyan, C.W. Outhwaite, Phil. Mag. B 69 (1994) 1051.
[9] L.B. Bhuiyan, C.W. Outhwhaite, J. Chem. Phys. 116 (6) (2002) 2650.
[10] C.N. Patra, A. Yethiraj, Biophys. J. 78 (2000).
[11] K. Wang, Y.-X. Yu, G.-H. Gao, G.S. Luo, J. Chem. Phys. 123 (2005) 234904.
[12] V. Vlachy, D.A. McQuarie, J. Chem. Phys. 83 (4) (1985) 1927.
[13] E. Raspaud, M. da Conceicao, F. Livolant, Phys. Rev. Lett. 84 (11) (2000) 2533.
[14] T. Das Bratko, L.B. Bhuiyan, C.W. Outhwaite, J. Chem. Phys. 107 (21) (1997) 9197.
[15] J. Blaul, M. Wittemann, M. Ballauff, M. Rehahn, J. Phys. Chem. B 104 (30) (2000) 7077.

[16] Y.-X. Yu, J.Z. Wu, J. Chem. Phys. 117 (2002) 10156.
[17] L. Mier-y-Teran, E. Diaz-Herrera, M. Lozada-Cassou, D. Henderson, J. Phys. Chem. 92 (22) (1988) 6408.
[18] M. Valisko, D. Henderson, D. Boda, J. Phys. Chem. 108 (2004) 16548.
[19] K. Hiroke, Mol. Phys. 33 (4) (1977) 1195.
[20] E. Gonzales-Tova, M. Lozada-Cassou, D. Henderson, J. Chem. Phys. 83 (1985) 361.
[21] G. Lamm, G.R. Pack, J. Phys. Chem. B 101 (1997) 959.
[22] J. Skerjanc, D. Kozak, S. Hocevar, G. Vesnaver, B. Jus, D. Dolar, Biophys. Chem. 6 (1977) 9.